Design and R&D on TEM-based Kicker Systems at SLAC

A. Krasnykh, B. Hettel, and J. Seeman

SLAC Linear Accelerator Laboratory, Menlo Park, CA

Abstract

SLAC National Accelerator Lab is a multipurpose laboratory today based on operations of two main facilities and one facility for accelerator technology R&D. They are accordingly SSRL synchrotron light source, LCLS x-ray FEL, and (future) FACET-II (Facility for Advanced Accelerator Experimental Tests). The injection and extraction systems for beams are needed in all mentioned above facilities and they are continuing to be developed according to the SLAC facilities evolution and updates.

Our note will review the results of our past and present experience on the TEM-mode kickers. We will discuss features for the advanced kicker structure proposed at SLAC in 2002. The proposed kicker concept was updated from different aspects including a cost effective manufacturability. A part of this R&D is linked with the study of high power bunch-by-bunch feedback kickers with the goal to develop a fully functional vacuum compatible structure to be installed in SuperKEKB facility.

Engineering aspects of multi MW peak power pulsers with pulse rise/fall/top in nanosecond ranges will be discussed too. R&D experimental results on the different pulser schemes and layouts and their performances will be presented too. A part of this R&D work is linked with the study of the LCLS-II beam line with a distribution closely spaced bunches to multiple undulators to take advantage of combining different colored x-rays. A development of the pulser critical components is based on a collaborative link with our national industrial partner (VMI, Visalia, CA).

Work supported by DoE contract DE-AC02-76SF00515.

This material is based upon work supported by the U.S. Department of Energy, Office of Science, under Contract No. DE-AC02-76SF00515.

A) Introduction

This SLAC R&D effort has been ongoing in the optimization of the TEM-kicker electrodynamics, from its bandwidth and the beam impedance reduction point view. This effort is supported by the SLAC–KEK US-Japan collaboration activity.

A reader could find many articles concerning the TEM kicker issues. The SLAC approach for consideration is based on a fundamental paper "Dynamic Devices: A Primer on Pickups and Kickers" written by D. Goldberg and G. Lambertson (AIP Conference Proceedings #249) [1]. The paper describes the basic electrodynamics issues of TEM-based kicker structures. A leitmotif of this note would be as follows: We have grasped a general view on these dynamic structures; let us do not by pass the details. This note contains many details which support the basic issues.

There was an R&D effort concerning new schemes based on the full swap out of the stored bunches that requires the development of the technology of fast kickers with short rise and fall time, long stable flat top, and reduced field ringing [2, 3]. The SLAC activity concerning on this issue was supported by a Memorandum Purchase Order that has been issued for the SLAC service of ANL in a frame of APS MBA-Upgrade. Recently there is a call for the R&D work that is linked with the study of the LCLS-II beam line with a distribution closely spaced bunches to multiple undulators to take advantage of combining different colored x-rays. In all the above cases the advanced TEM kicker structure and the multi MW peak nanosecond pulser are key components for the R&D effort.

The dynamic experiments in the MaRIE project [4] will require series of micro-pulses that can be irregularly spaced within the macro-pulse of an X-ray FEL, and these patterns can change from macro-pulse to macro-pulse.

In all the above cases the advanced TEM kicker structure and the multi MW peak nanosecond pulser are key components for the R&D effort.

B) Electrodynamic effects of the PEP-II Original and Upgraded TEM Kickers

The advanced TEM-mode kickers for modern installations require R&D effort- because the kicker design must take on the difficult challenge of stably colliding low-emittance, short-lifetime, and high-current beams. The high average circulating beam current is based on an employment of trains of shorter bunches, trains with a shorter period between neighboring bunches. Such bunch trains produce the effects in the kicker structure which have not covered in the cited paper above.

In the past SLAC and LBNL have designed and built high-temperature feedback kickers for the PEP-II B-Factory that have withstood more than 3.2 A of circulating positron current without damage. The transverse feedback kicker (TFB) structure is shown in Figure 1.

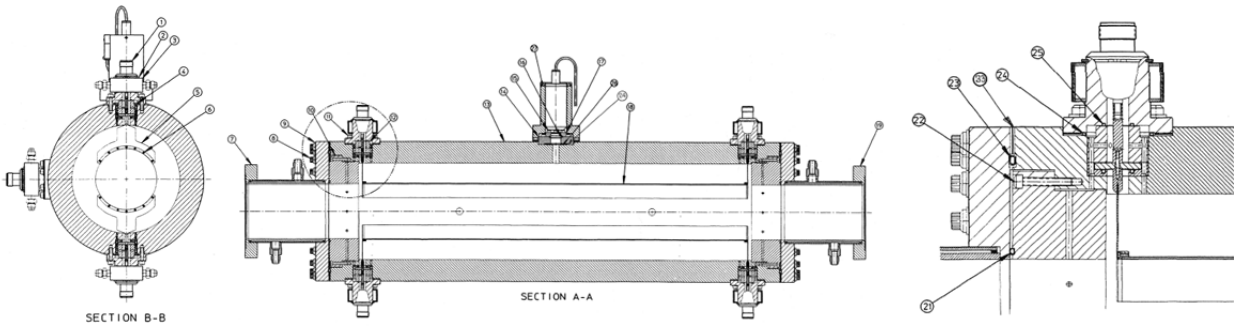

Figure 1: TFB PEP-II kicker, front and longitudinal cross sections with detailed feedthrough port on the left

The designed specification is shown in Table 1 [5].

Table 1 PEP-II LER tranverse feedback kicker specifications

Parameter	Description	Value
E	Beam energy	3.1 GeV
f_{rf}	RF frequency	476 MHz
I_b	Average current	3.0 A
f_0	Orbit frequency	136.3 kHz
β_{av}	Average β	10 m
ν_f	Fractional tune	0.9
τ_b	Bunch spacing	4.2 ns
Z_{rw}	R-wall impedance	4.85 MΩ/m
α_0	Growth rate of m = 0 mode	3200 sec^{-1}
$\partial V/\partial x$	Req'd feedback gain	14.6 kV/mm
R_s	Kicker shunt impedance	24 kΩ
P_k	Available kicker power	240 W
V_{max}	Max. available kick	3.4 kV
y_{max}	Max. mode amplitude	0.23 mm
V_{mode}	Voltage to excite y_{max}	71.3 kV-turn
Δf_{min}	Req'd bandpass	13.6 kHz-119 MHz
–	Electronics bandpass	10 kHz-250 MHz
–	Kicker bandpass	DC - 119 MHz
σ_y	Vert. beam size	0.16 mm
-	Req'd dynamic range	23 dB
-	Actual dynamic range	42 dB
y_{os}	Allowable effective orbit offset	1.8 mm

Let us review the kicker details that are important for a modern design.

- Detail #1

A transverse feedback (TFB) system from PEP-II experience shows that the existing kicker structures are limited in operational bandwidth. For example, Figure 2 illustrates the beam induced HOM power (in dB) extracted from the TFB kicker vs. frequency.

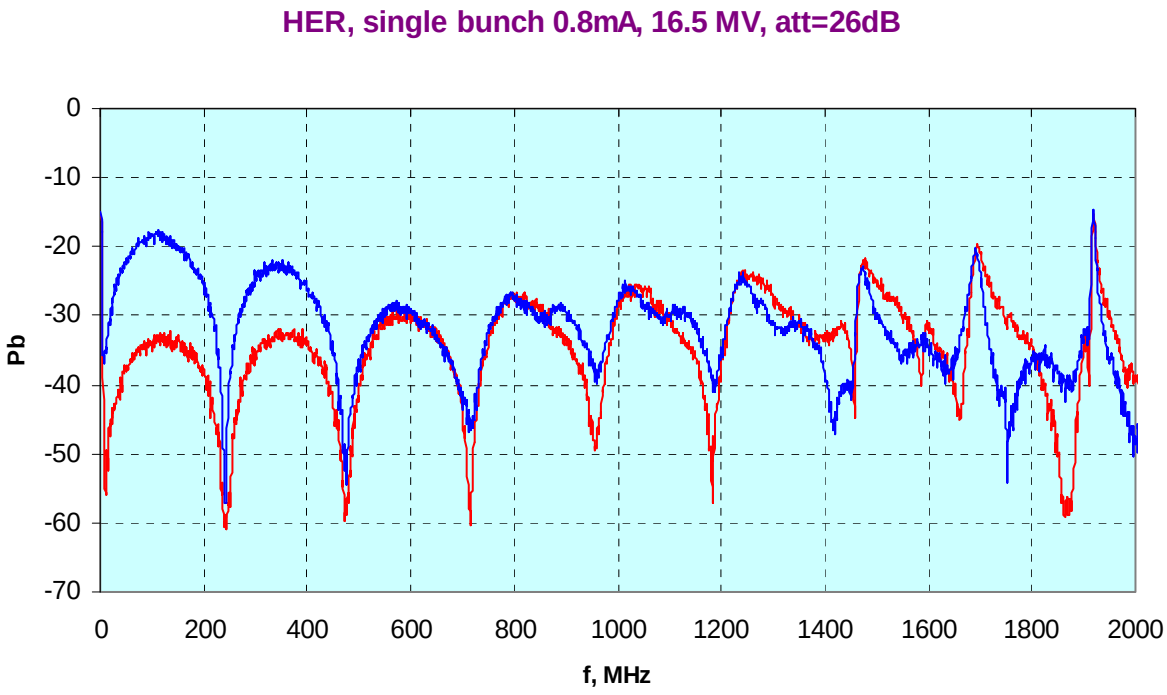

Figure 2: HOM spectrum in PEP-II. The blue trace is the beam induced power that goes to the kicker load and the red trace is the beam induces power that goes to the TFB amplifier (HOM power measurement at single kicker electrode)

There is a good kicker directivity (~15 dB) at 0 < f < 500 MHz frequency range and there is there is a directivity absence in f > 500 MHz.

- Detail #2

The bandwidth (BW) limitation is a problem in two ways: (1) the BW limitation is a source of heat due to the beam HOM absorption (and a relatively poor heat extraction from the kicker stripline structure) and (2) there is a potential problem to damage the RF feed through and the TFB RF source/amplifier.

- Detail #3

There are two major components which limit the kicker BW: (1) a vacuum feedthrough region and (2) high RF power terminating loads. A typical BW for a vacuum tight and bake-able feedthrough is limited by 1-2 GHz. Figure 3 shows the impedance discontinuity along to feedthrough for a bake out vacuum feedthrough (for an illustrating purpose).

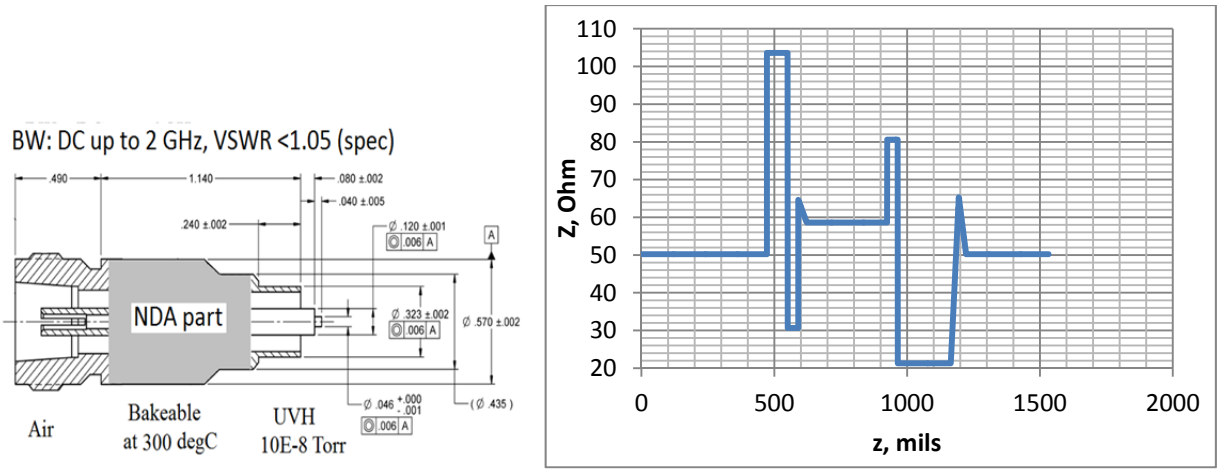

Figure 3: Vacuum feedthrough cross section and impedance discontinuity along the feedthrough

The bunch spectrum in modern installation is much wider and prolongs up to 10 GHz. For example, a σ_z=5 mm bunch length corresponds to the σ_f=9.4 GHz Gaussian width of a bunch in the frequency units. The feedthrough acts as a bandpass HOM filter and allows the beam HOM power to remain in the kicker structure. The current fabrication technology of the vacuum tight feedthroughs limits the BW rather narrowly for advanced accelerator technology demands and this fact forces us to find an adequate R&D solution and sponsor. The BW limiting issue is worse for a multi MW peak case.

- Detail #4

Let us assume that there is a technical solution for the feedthroughs and the HOM power is extracted from the existing kicker structure, the BW of which is limited by the current design. The HOM power will be extracted from upstream and downstream kicker ports due to their directivity. The question is whether a coax cable can handle with this power or not. For example, a max RF loss/ft for the LDF4 cable from Andrew Incorporated should be limited to 6 W per foot (20 W/m). The size of the cable must be taken in an appropriate way. The next components are a TFB amplifier (or a pulser) and a power terminating load. Our TFB experience at PEP-II shows that the output of a solid state RF amplifier is sensitive to a level of the extracted HOM power. A typical configuration of the amplifier based on several RF cells the power of which is combined on an output port. The low voltage RF transistors are employed in cells. The HOM power can have an effect on operation and protecting components are necessary. Filtering of the HOM induced power is possible if the kicker source frequency range is much lower than the HOM frequency range. Figure 4 shows a layout of the kicker structure with the HOM filter.

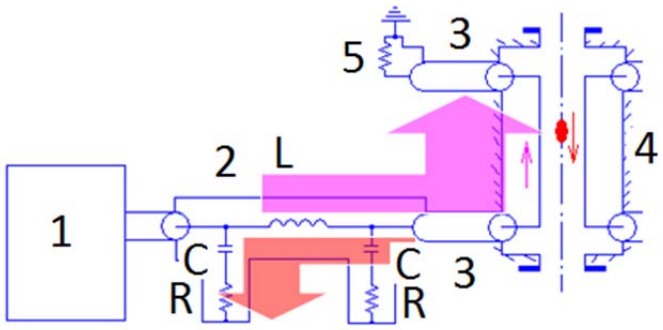

Figure 4: Layout for main components of the kicker system. 1 is the kick source, 2 is a HOM filter, 3 is a feeder, 4 is a kicker structure, and 5 is a terminating load. The pink arrow illustrates the direction of the kicker pulse flow and the red arrow shows the direction of the beam HOM power

However there are several issues that must be resolved:

- What a realistic level of residual energy is between bunches with HOM filters?
- The electric field pattern of residual power vs. the bunch pattern.
- Where the optimal position of HOM filter should be placed (in or out of tunnel)?
- What the optimal filter parameters (LCR) are? How they are realized (engineering problem)?

The same layout was used in the PEP-II TFB system. Homemade bandwidth filters were employed. A critical component is filtering capacitors (C). These components must hold off the HOM power and in the same time do not shunt the kick power. A voltage hold-off of low inductance RF capacitors actually less than a 50 VDC. The HOM power loss in capacitors produces a heat. The induced voltage level and temperature may result in a failure mode. There were several failure incidences for the PEP-II TFB filters (see Figure 5).

Figure 5: Event of the HOM filter failure in PEP-II.

One can find more details in [6]. Let us go back to the kicker structure to describe other details.

- Detail #5

As it was shown above the high current beam train HOM power may live or remain in the kicker producing heat in the structure. This effect is traced to the poor mode matching and the BW limitation on the kicker ends. The heat removed from aluminum alloy kicker electrodes is challenging. This leads to

elevated temperatures of the aluminum electrodes and was ultimately a limit for the storage beam current [7]. New electrodes were designed for the transverse feedback kickers that are expected to extend the current range of the LER well beyond 3 Amperes. Molybdenum (Mo) has been chosen because of its superior thermal properties and the ability of achieving good radiative cooling by simply oxidizing the surface in air at 530degC.

- Detail #6

However, the Mo density in higher compared to an Al-alloy density. It was found that the electrode of the horizontal kicker had sagged down by a few mm, due to the increased weight of the Mo electrode compared to the original Al-alloy electrode and the cantilevered support of the electrodes by the feedthroughs. Figure 6 shows a gravity effect of "heavy-weight" Mo-electrodes.

Figure 6: a) Mo-electrode assembled with paddle and central pin, b) Gravity force bends feedthrough pin and breaks the axial symmetry.

The remedy of this sagging effect was to add Macor pins to the "paddle" structure holding the electrode in place; these pins engage into openings in the end caps of the kicker housing. Figure 7 illustrates this idea.

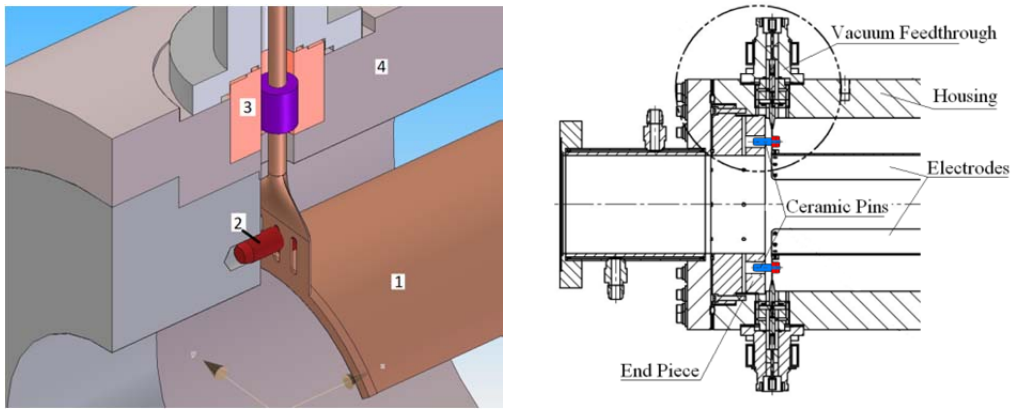

Figure 7: 3D view at the upgraded PEP-II kicker end. 1 is a Mo-electrode, 2 is a pin, 3 is a support assembly, and 4 is kicker housing.

Initially, the modified kicker performed well with measurements confirming that the match at the ends had not deteriorated in any measurable way. However, as beam currents were increased, and during a

period of relatively high bunch current, vacuum spikes were observed in the pumps near the kicker. Reanalysis of the kicker structure revealed the most likely scenario of failure. When a bunch with current I_b travels through the kicker, it gives up some of its energy to that structure. The energy loss may be expressed as a voltage V_{loss}, and the beam impedance $Z_{||}$. The simulated beam impedance spectrum in the structure and the measured induced beam power from the kicker are shown in Figure 8 and 9 accordingly.

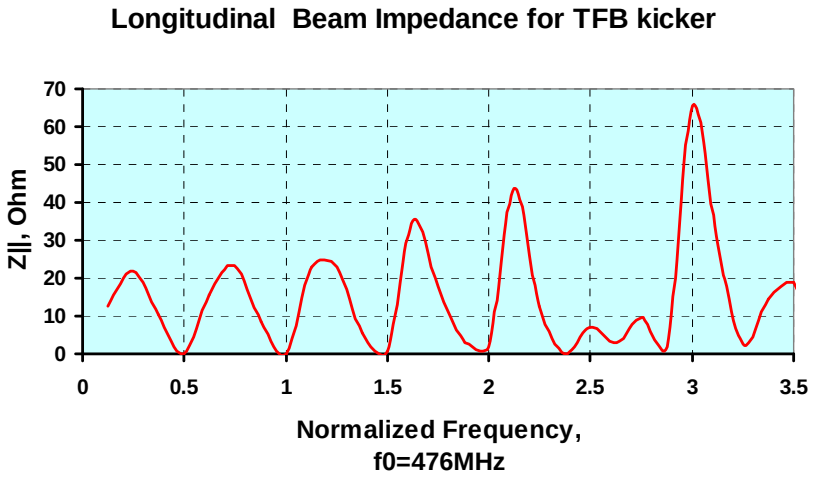

Figure 8: HFSS simulation of longitudinal beam impedance vs. frequency in PEP-II with the improved transverse kicker. The average kicker beam impedance is $Z_{||}$=34 Ohm for the 59.5-1700 MHz frequency range.

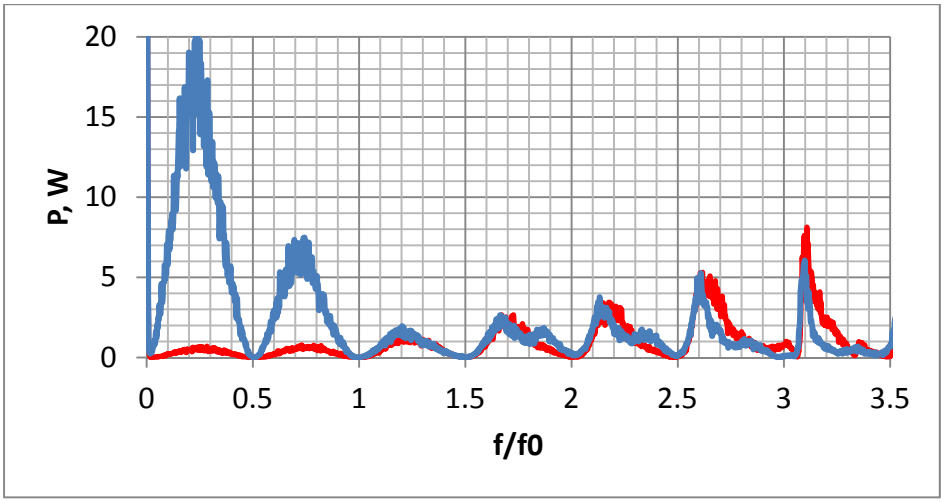

Figure 9: Beam induced RF power measurement from upstream (blue trace, load) and downstream (red trace, amplifier) kicker ports vs. frequency. Measurements were performed on one kicker electrode

First, the reader can see a discrepancy in the 2.5 < f/f0 < 3.0 range. This discrepancy is understood but it is not a subject for the current detail discussion here. When evaluated at low frequencies using the average beam current, the expected voltage to ground in the region of the mounting paddles is on the order of 100 V and, thus, no danger of arcing exists. However, with bunch length of about 12 mm the

peak beam current in fact approaches 100 A (for 3A average beam current) and in addition the wider impedance spectrum shows impedance peaks of near 250 Ohm (see Figure 10) at frequencies higher than 2 GHz, where the beam current still has significant spectral power that has been left in the structure.

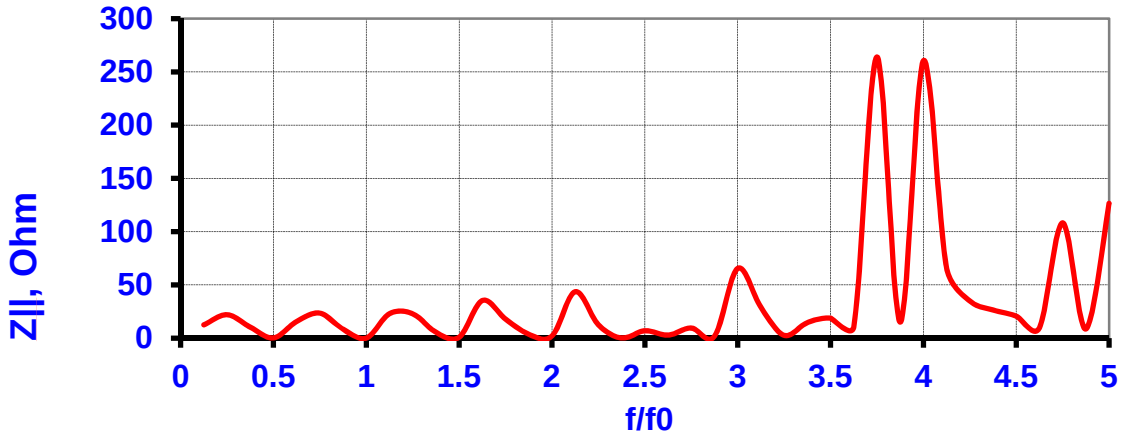

Figure 10: Wide frequency range for longitudinal beam impedance for modified kicker

For the 1 cm long bunches peak currents exceeding 100 A, a modest impedance can give rise to voltage spikes and discharges. A potential surface breakdown is likely to take place.

- Detail #7

A comparison of the beam induced HOM power spectrum for the 2.2 < f [GHz] < 7.2 frequency range for modified (horizontal) and original (vertical) kickers is shown in Figure 11.

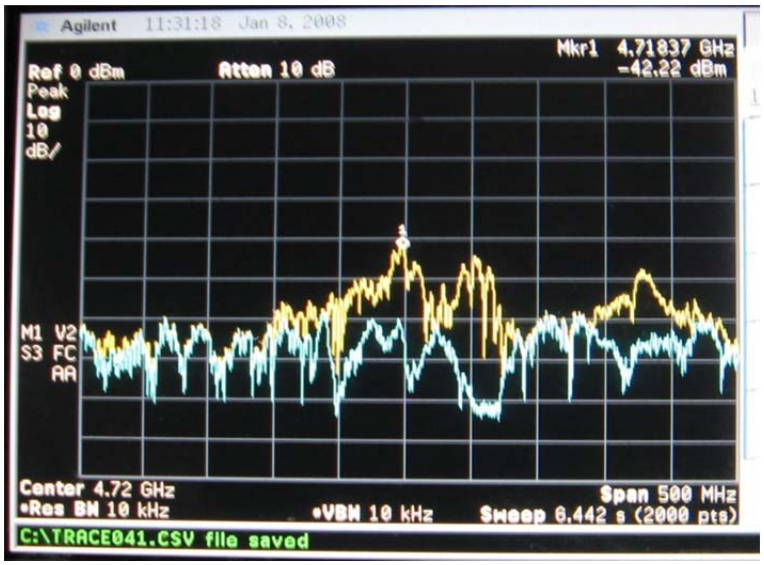

Figure 11: HOM beam power extracted from modified (a yellow trace) and original (a blue trace) TFB kickers

Only a qualitative analysis of a HOM field pattern is possible from this spectrum because there is a BW limitation in this feedthrough transition region. Analysis shows that the first trapped mode belongs to transition between the pin and a capsule. The capsule is a power transmission region between the

vacuum feedthrough and the kicker electrode. The half-length of this region is 3.16 cm and this half-length relates to 4.72 GHz as it is shown in Figure 12a. There are other frequency peaks in the spectrum for modified kicker structure. The next frequency peak at 5.2GHz with a wavelength λ_2=5.76 cm corresponds to the length of kicker electrode arc. The following frequency peak at 6.47 GHz (λ_3=4.63 cm) corresponds to the length of an arc between kicker electrodes. These wavelengths are shown in Figure 12b.

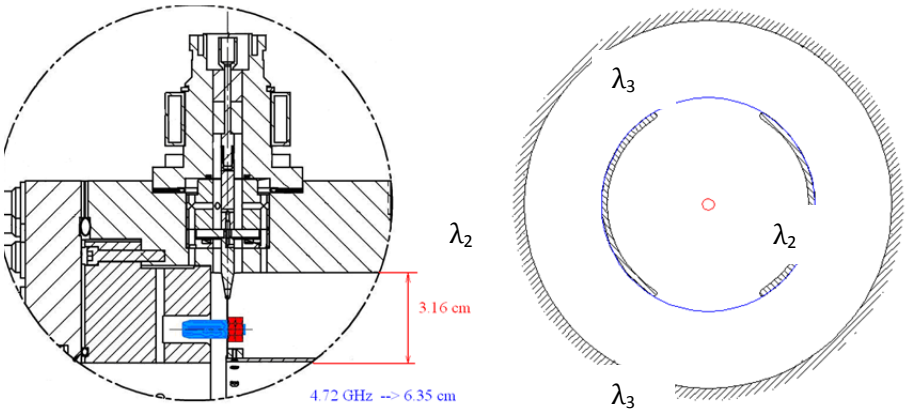

Figure 12: a) Kicker end cross section, b) cross section of the kicker front view.

The pins installed for mechanical stability turned out to be a weak spot causing discharges (Detail #6) and provoked a section that trapped modes in the kicker end region (Detail #7).

- Detail #8

This paragraph describes a BW limitation of the commercially available high power loads and attenuators. As an example, a 1 kW air cooling attenuator assembly is shown in Figure 13.

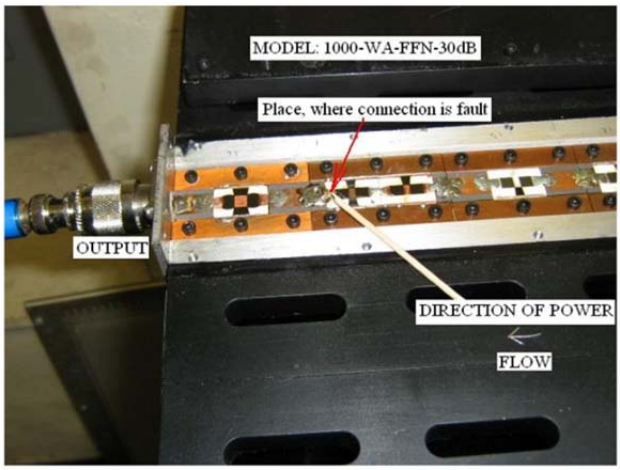

Figure 13: Final stages of a 1kW air cooling attenuator assembly

A specification for the voltage standing wave ratio shows that VSWR=1.1 from DC to 1.0 GHz and VSWR=1.25 for 1.0 GHz < f < 2.4 GHz frequency range. A bipolar BPM signal pulse width (see a blue waveform in Figure 14) is almost 400 psec. It corresponds roughly one cycle of a 2.5 GHz.

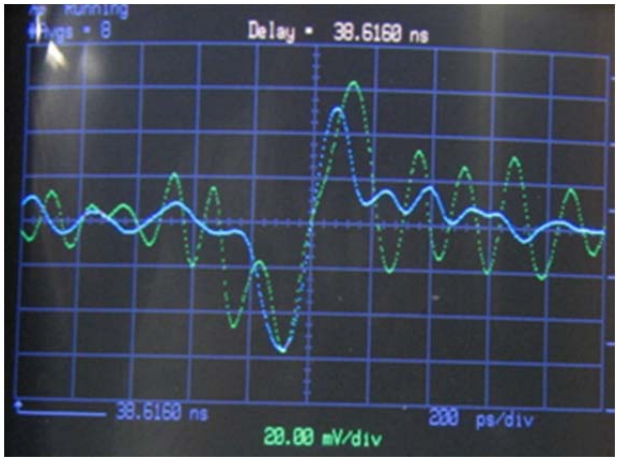

Figure 14: Transmission of a 2.5 GHz mono-pulse through a 1 kW attenuator

The green trace shows a distortion of the BPM signal at the output attenuator port. There is an oscillation even after 1 nsec. This fact indicates several things: (1) due to the BW limitation of the high power load there may be bouncing HOM power in the feeder, (2) the VSWR specification does not give enough information concerning the duration of a transient process, and (3) an additional effort or study is necessary to specify a HOM termination issue.

Typically high power RF attenuators and loads contain an array of planar fixed chip 50 Ohm attenuators (see Figure 15).

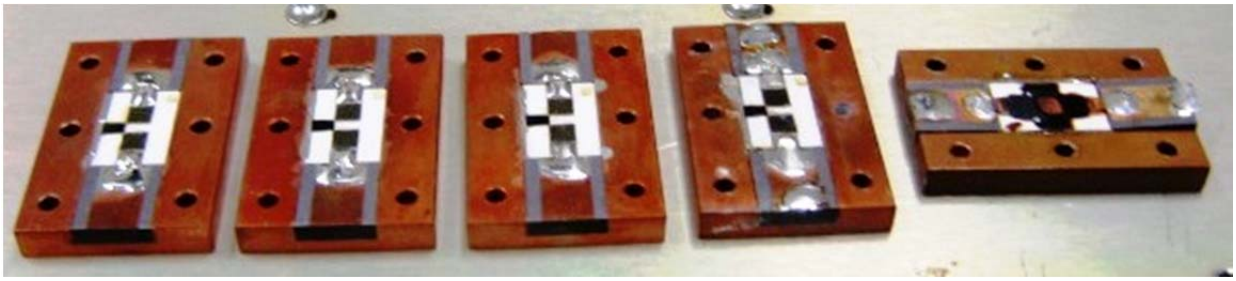

Figure 15: T-type schematic chips with different attenuating rates

An applied input voltage on a chip is limited by a 100 VDC only. An over voltage in the short nsec pulse mode is possible but the chip lifetime in this mode will be reduced.

Barth Inc. is a vendor for broadband high voltage attenuators [8]. The spec of the Barth 50 Ohm attenuator (model 2536) indicates a wideband range from DC to 10 GHz and a maximum input voltage from 7 kV peak to 60 kV peak depending on the FWHM pulse. The average power is limited by 200 W. An employment of this type of attenuator in the advanced kicker system is a subject for evaluation in the future.

There is an array of other “details” of the kicker system components but we shall not describe them here and shall describe the advanced kicker structure that has been proposed at SLAC on the end of 2002.

The reader could be confused why a 15 year old proposal was not realized earlier. There are several reasons for that. The advanced kicker proposal was born after the PEP-II B-Factory was put in the commissioning and operation mode. With operating budget limitations, a priority was placed on luminosity and a limitation on the HEP lifetime dictated to optimize the machine that as build. However this strategy allowed to gain extended knowledge of our existing kicker system and to implement our potential upgrades for further programs.

Basically there are two major regions in the TEM kicker structure: (1) a regular part where there are kicker electrodes are inserted in the housing/body, and (2) kicker ends where there are coaxial vacuum feedthroughs connect with electrodes and there are duct pipes for a bunch passage. Beam pipe discontinuities are a source of the HOM power left in the kicker after the bunch passes through the structure. Two basic types of TEM kicker structure are shown in Figure 16.

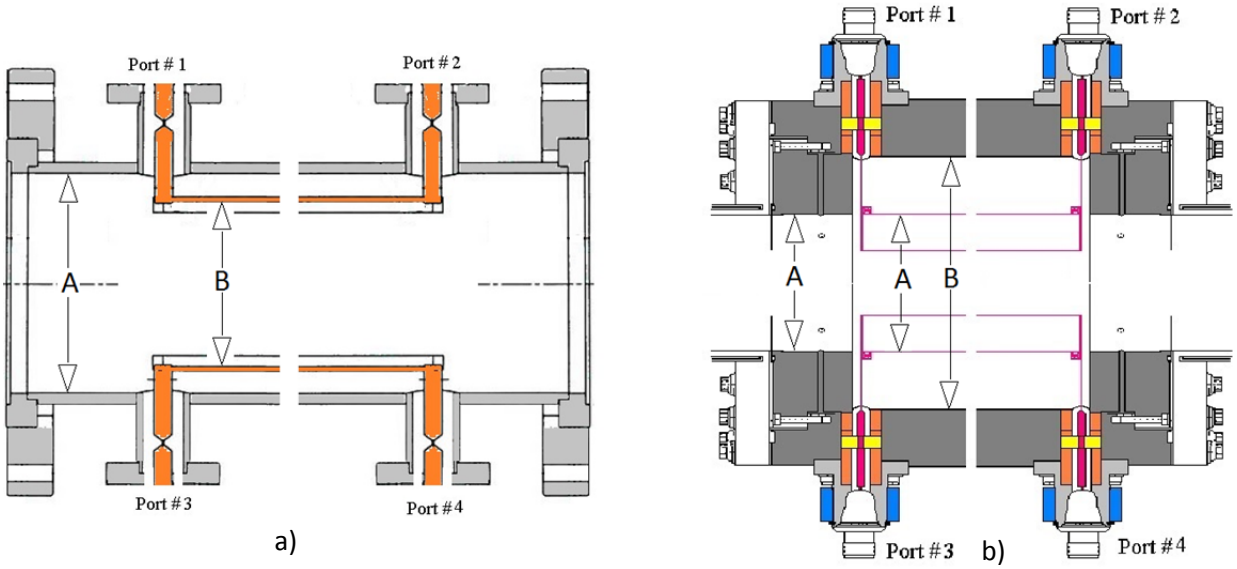

Figure 16: a) Kicker housing with 'A' beam aperture equal to the beam duct (there is no a discontinuity in the beam line), b) The 'B' inner diameter of the kicker housing is larger than the A diameter of the beam duct.

The a) and b) kicker layouts were employed in the KEK and SLAC B-Factories accordingly. A comparison of the longitudinal beam impedances for these structures is shown in Figure 17. As it is seen from this picture the beam impedance of the KEK TFB kicker structure is less by a factor 3 for the same frequency interval. However, the electrode coverage factor for the SLAC structure is two times bigger. Actually, a uniform kick area is wider for structures with larger electrode coverage factors. The KEK kicker structure is less sensitive for the trapped HOM mode. The frequency cutoff for the SLAC TFB kicker design is reduced compared to the KEK TFB one. SLAC TFB electrode-to-coax transmission part is rather complicated and contains an array of discontinuities. This fact makes difficulties of the HOM power extraction from the vacuum kicker components. This fact also effects on direct HOM power measurements on the kicker ports. A coupling coefficient between the HOM power inside of the housing and the 50 Ohm ports may be less than 1.0.

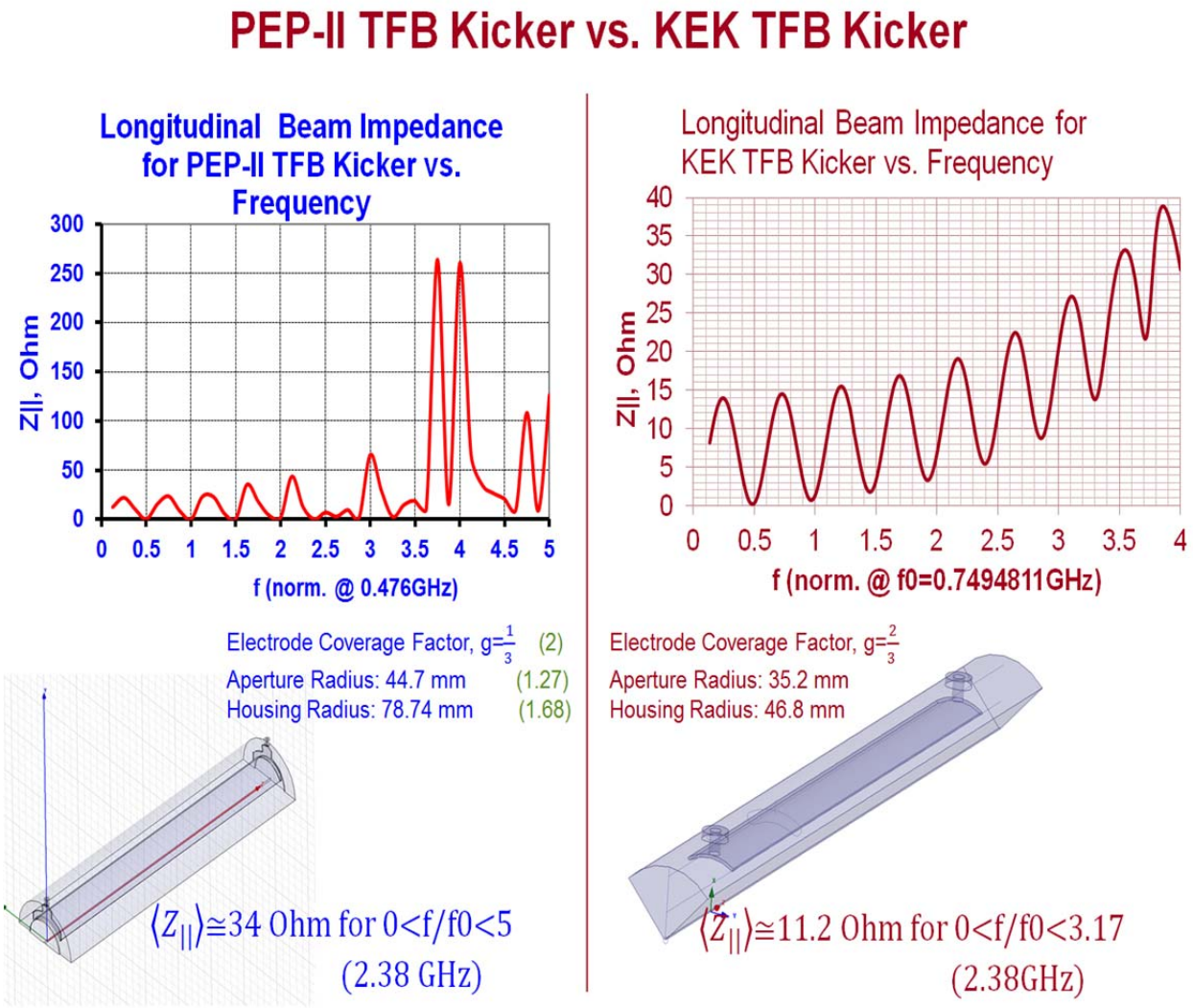

Figure 17: Comparison of beam impedances for SLAC and KEK TFB kickers.

C) New Transverse Kicker Design

- Detail #9

This paragraph illustrates an importance of a kicker end shape optimization. One can see that the SLAC TFB kicker end shape is rather complicated compared against the KEK one. The bunch electromagnetic fields are perceptibly deformed in both SLAC and KEK TFB kicker ends. For example, Figure 18 illustrates the electromagnetic field variation along two lines. The Line #1 is a line where 0 < r < R_electrode and the Line #2 (blue solid lines) is a line R_electrode < r < R_housing, where R_electrode is a radius of the kicker electrode, and R_housing is the inner radius of beam vacuum duct.

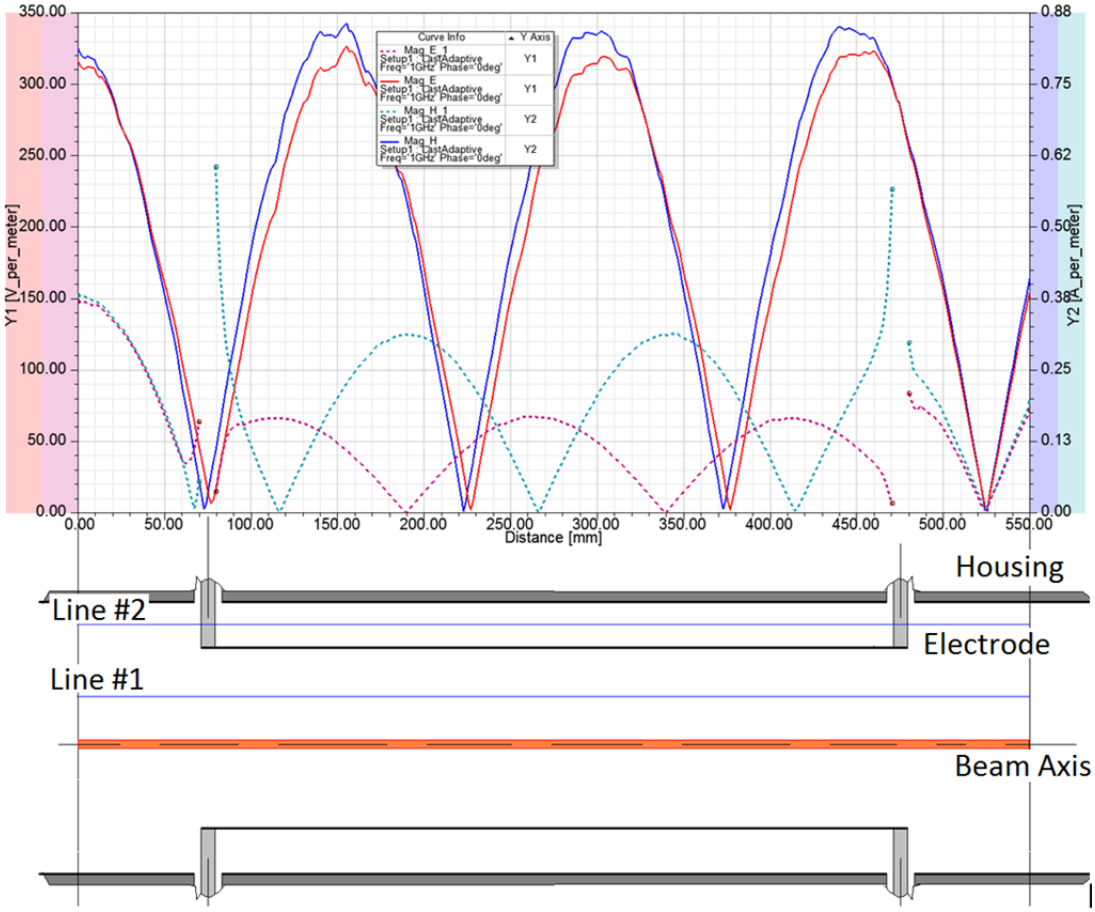

Figure 18: Electric (E, red color traces) and magnetic (H, blue color traces) fields at 1 GHz along the KEK kicker structure. Solid and dot traces are for EM fields along Line #1 and # 2 accordingly

One can see a phase synchronization EM fields along Line #1 and #2 of on the right and left sides of the kicker structure. However E and H are still in phase along Line #1 but the phase between E and H is shifted (by 90deg) only along the kicker electrodes. The E and H phase synchronization is broken at the left kicker ports and the phase synchronization is restored on the right kicker ports. There is a phase synchronization of the beam induced EM signal on the left kicker ports (a mono polarity pulse shape) and there is a two-polarity pulse shape on the right ports. The phase shift between E and H components explains why the downstream port signal has a bipolar form. Figure 18 illustrates the EM field variations at 1 GHz. However, the kicker ports perturb the bunch HOM fields for all frequencies of a spectrum. The goal of kicker design is minimize this perturbation.

For the past few years we have been working with KEK collaborators studying the possibility of adapting SLAC PEP-II's high-current strip-line kicker design to SuperKEKB with modelling, prototyping, and then building a full vacuum-compatible unit to be installed and tested.

SuperKEKB plans to operate with nominal beam currents of 2.6 A electrons and 3.6 A positrons at bunch lengths down to 5 mm (σ_t=17 psec, σ_f=9.4 GHz) and bunch spacing of 4 nsec. The SuperKEKB beams will severely tax the power-handling ability of the feedback kickers for the bunch-by-bunch feedback

systems. A stable and reliable mode of operation in such an environment dictates a careful consideration of the beam impedance budget and the related HOM power deposition and HOM trapped modes. The small budget of impedances is necessary for the beam dynamic and the bunch-by-bunch transverse feedback kickers. The next problem is connected with the 4 nsec range of the bunch spacing and the long bunch train and the resonant buildup of mode power. Any residual energy left in the beam line couples to the HOM loads. This proposal will address this study and development of the stripline system for modern facilities specifically the KEK SuperKEKB storage ring e+e- collider.

A new stripline approach was proposed at SLAC in 2002 and contains ground fenders, tapering electrodes, and stripline end HOM absorbers.

In detail, the TEM kicker structure contains two matched tapered regions (ends) with grounded fenders which improve the matching between odd and even modes. This feature makes the impedance a constant and broadband. Additional to this, the ground fenders will reduce the longitudinal beam impedance. That means that less HOM power will be left in the structure when bunch passes by its.

The tapered ends of the stripline make the kickers a little longer. However, the beginning of the tapering edge will minimize a perturbation of bunch electromagnetic fields. The length of tapering part (and other lengths and dimensions of kicker components) is not arbitrarily set. The length chosen is based on the HOM beam harmonic frequency. At the kicker ends are HOM absorbers that are brazed onto the water cooled ends. The absorber material must be chosen to improve power loading, material resistivity, bake out, and heat emissivity. Figure 19 is a slide where the major components for advanced kicker are shown and when and where the advanced SLAC structure was discussed.

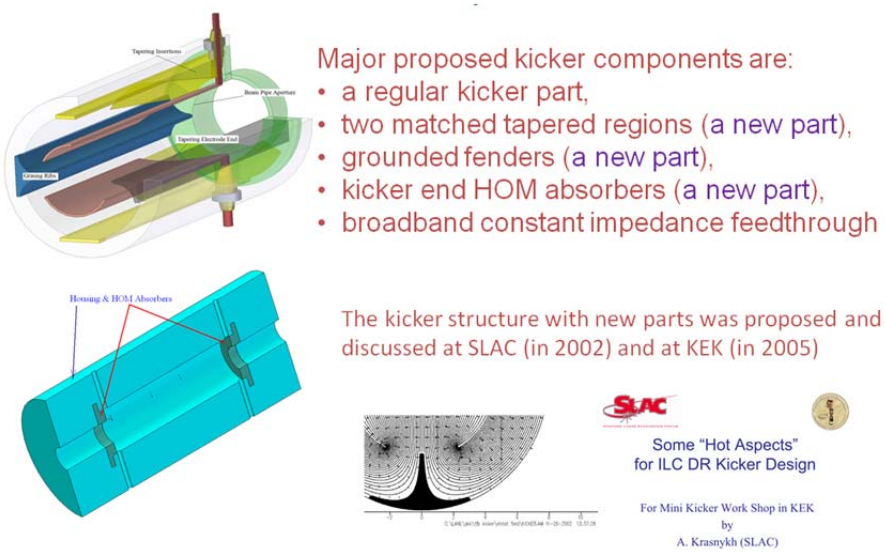

Figure 19: Employment of matched taped regions, ground fenders/ribs, and HOM absorbers make the kicker structure capable to operate with a high storage current and short bunch length.

Figure 20 shows some details of the proposed kicker structure.

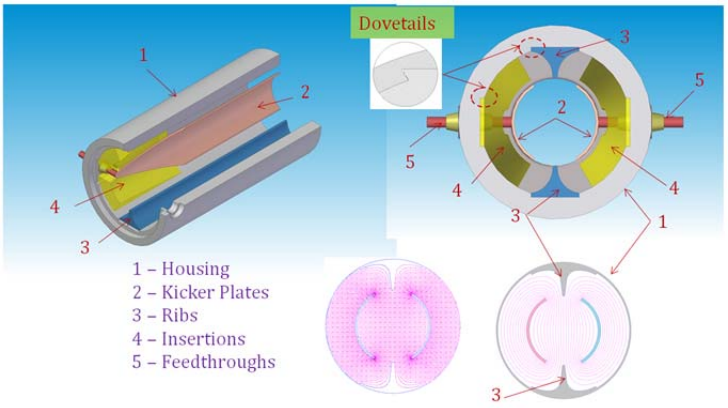

Figure 20: Components of proposed kicker structure.

The perturbation of the bunch induced HOM fields is minimized at a vicinity of the central pin feedthrough and kicker electrode connection. The ground fenders are uniform along the kicker structure. However further optimization area/space between insertions (4) and fenders (3) are needed. The insertions (4) may perform as a HOM absorber if the electric and thermal conductivities are properly chosen. Our preliminary analysis shows that carbon/carbon-silicon carbide composite can be acceptable materials for this insertion.

It is important to simplify the advanced design in order to have a cost effective mechanical solution. Figure 21 illustrate a proposed assembly steps for the advanced kicker.

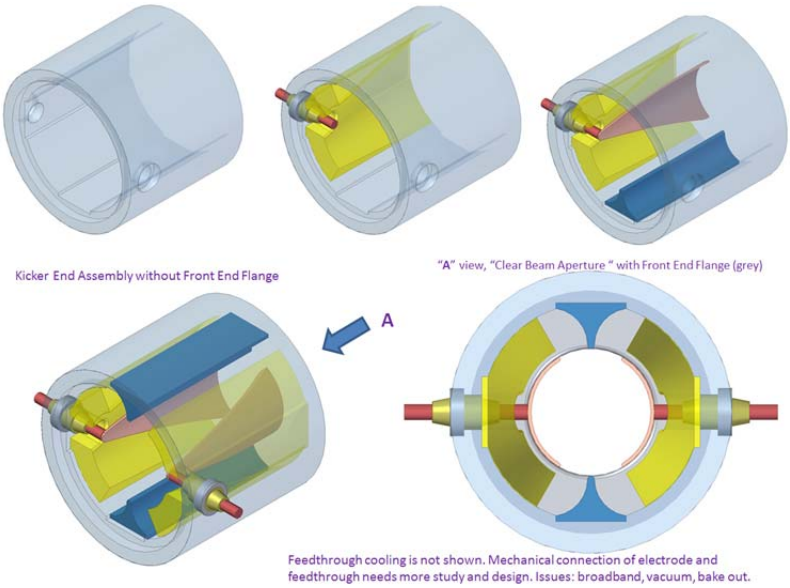

Figure 21: Assembly steps: Step 1 is the housing without components, Step 2 is the housing with insertions and feedthroughs, Step 3 is mounting of the kicker electrodes and ground fenders, and in final Step 4 the front end flanges are assembled.

Although the advanced kicker has been discussed at SLAC many years ago the proposal is still in beginning phase as "a white paper". There needs to be further engineering considerations, a prototype built, and drawings made for fabrication.

D) Power Supplies for Nanosecond TEM kickers

Transverse feedback kickers:

Power supplies for the TFB TEM kickers are broadband high power amplifiers. Their BW typically correlates with the RF harmonic frequency of a main storage ring RF source. For example, a 1 MW CW 476 MHz (λ_0=63 cm) klystron amplifier was employed in the SLAC PEP-II B-Factory. The TFB port-to-port kicker length (electrode lengths) is 63 cm accordingly. That means that there is a 2.1 nsec transit time of the kick wave propagates in the structure. In order to produce a more powerful kick (to use both: a transverse electric and magnetic components of wave), the kicker is fed from downstream ports; so twice the propagating time (4.2 nsec) is needed for it to effectively work. This fact actually requires a highest level for a supporting electronic bandpass which is 119 MHz. Broadband solid state amplifiers are used in the TFB systems. Their maximal output power lies in a kW scale. That indicates that an effective voltage in the 50 Ohm feeder is limited by several hundred volts. Accordingly requirements for the kicker components (e.g. feedthroughs, cables, connectors) are not the same as the requirements for the components of injection/extraction TEM kickers.

Multiple beamline kicker pulsers:

Multi MW peak power pulsers with pulse rise/fall/top in the nanosecond range are requirements for new schemes based on the full swap out of the "bad" bunch in the train of stored bunches and replace it by a "good" new one. The similar pulser requirements also are discussed for the study of the LCLS-II beam line with a distribution closely spaced bunches to multiple undulators to take advantage of combining different colored x-rays. Modern XFELs based on CW-mode superconducting GeV linacs need a distribution system that could controllably direct bunches into different undulators. Although a separation between bunches can be approximately 1 microsecond simple and reliable nanosecond pulsers would be attractive for such distributing system. Overview of driver technologies for nanosecond TEM mode kickers was discussed recently [9]. In this paper we will discuss some details and challenges. We will consider a conventional pulser layout i.e. with a 50 Ohm of the pulser output and the feeder impedance accordingly and a multi MW peak output power. We also limit ourselves with a pulse width less than 50 nsec i.e. a case that a direct employment either fast thyratrons or solid state switches is challenge. For sure there are different engineering approaches to achieve the above course specifications: for instance, directly design a triggered spark gap etc. In addition, designers are looking for a cost effective way to solve a problem.

It is known that industrial powerful switches (such as gas filling tubes and IGBTs) possess the following feature. The current rise time through the switch is longer vs. higher switching current amplitude. It is not possible to get the rise time shorter than 40-50 nsec for multi MW peak at 50 Ohm resistive load via available components from the industry. A common feature of all industrial available high power

switches indicates that the current rise rate is reduced with increased amplitude of the switching current.

Industrial pulser components:

It is known that the non-linear transmission line (NTL) behaves in an opposite way: a current rise rate is an inversely proportional of the acting current amplitude. The NTL can assist the industry available switches to get a high di/dt on a 50 Ohm load. Theory and engineering issues for a NTL design was developed in 60th [11]. This book was in Russian. However, the book "Pulsed Power" by G. Mesyats (ISBN 0-306-48654-7, eBook) [13] in Chapter 21 contains the Shock Wave (SW) theory and basic circuit layouts. As follows from theory and experiments a structure of the initial wave (that propagates through the NTL) contains a regular and a shock electromagnetic part. The regular electromagnetic wave is a wave with a shape or profile of which practically does not change while the wave propagates through a transmission line. The SW is a wave the shape/profile of which depends on levels of the propagating current in the transmission line. A group velocity of the regular electromagnetic wave is $v_0 = \frac{c0}{\sqrt{\varepsilon_{eff}}}$, where c0 is speed of light and ε_{eff} is the effective dielectric constant. Spin reversal processes of the ferromagnetic media take place at the front of the wave only. A group velocity of the shock electromagnetic wave is $v_{sh} = \frac{c}{\sqrt{\varepsilon_{eff}\mu_{sh}}} = \frac{v_0}{\sqrt{\mu_{sh}}}$, where μ_{sh} is the effective permeability of a ferromagnetic media in the transmission line. The SW propagates in $\sqrt{\mu_{sh}}$ times slowly versus the regular wave. The impedance on the front shock wave is higher in $\sqrt{\mu_{sh}}$ times vs. the impedance of the line where spin reversal processes are completed. The front of the SW is in inverse variation with a magnetic field and a current accordingly. A difference in the velocities and impedances allows compressing of the electromagnetic power in the time while the wave propagates through the NTL. The compressing allows using the "slow" initial switch, i.e. assist a primary switch to get of a higher di/dt rate.

We would like to point out here several details which limit the SW assistance.

- Detail #10

A "strong limit" of the SW formatting is: air ionization and a partial discharge of voids, air pores, other "electrically weak" includes which were formed during a NTL fabrication. Ferrite cores are rather "electrically weak" ceramic and contain a conductive ferromagnetic material surrounded low conductive (isolating) oxide layers. Basically, a degree of a population or size of the ferromagnetic seeds against the size of oxide layer effects on the ferromagnetic material spec. A rise time of the SW (its front) in a transmission line with ferrite cores will be faster (shorter in time) if the reversal magnetic field in the line is higher. Other words, a higher current in the transmission line will create a shorter front. This fact indicates that a high voltage is necessary to apply in the line. High gradients in the transmission line can produce partial discharges. A slow component on the SW front just before the high dI/dt (dV/dt) may be a result of the partial discharge. A careful technology of a transmission line fabrication is needed.

- Detail #12

A ferrite material under the action of high electric gradients in a nanosecond range possesses an aging process. R. Haller [10] experimentally measured an aging curve (a number of pulses before breakdowns) for the ferrite material in a nanosecond range.

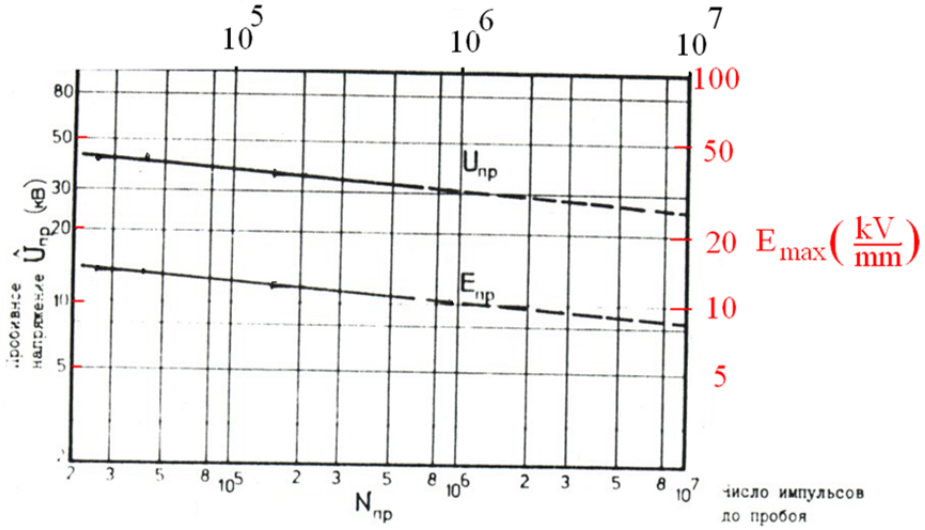

Figure 22: Aging of the ferrite materials under action of nanosecond pulsed power. The horizontal scale is a number of the nanosecond pulses before breakdown

- Detail #13

This detail is just a remainder that a ferromagnetic material will lose ferromagnetic features if a material temperature approaches to the Curie temperature. A repetition rate will be limited by the power dissipated in the ferromagnetic. A SW operation mode of the ferromagnetic material bears specific features and in some cases the short term R&D needed to meet the pulser specifications.

E) Pulser work at SLAC

There was R&D accordingly at SLAC in the past concerning to development of multi MW peak nanosecond pulsers in a period from 2006 to 2007. At that time Diversified Technologies, Inc. (DTI), under a SBIR grant from the U.S. Department of Energy, was developing a driver for TEM strip-line kicker damping rings of the International Linear Collider (ILC). The prototype pulser produced 5 kV peak pulses into a 50 Ohm resistive load, which otherwise would be satisfy the ILC requirements, as a precursor to the full 10 kV system. Because of the high 3-MHz pulse rate required, this design has to employ an all-electronic, rather than magnetic, approach to pulse formation. An analysis the pulser spec showed that driver based on the assistance of high voltage DSRDs (Drift Step Recovery Diodes) would be a cost effective engineering solution. However, a technology of DSRD-based pulsers was developed in the former USSR and was not widely known in the Western Europe and in the USA. One of the authors (A. Krasnykh at SLAC) was familiar with the DSRD technology and had a good relationship with the DSRD inventor. DTI employed Dr. A. Krasnykh (SLAC) and Dr. A. Kardo-Sysoev (Ioffe PTI, St. Petersburg, Russia, the DSRD inventor) as consultants and coordinators to design the pulse driver based on the DSRD approach.

Main result of this activity on the end of the DoE Phase II SBIR grant was to transfer the samples using DSRD technology fabrication to Voltage Multiplier, Inc. (VMI), Visalia, California. A VMI technology of high voltage diodes is, thus, similar to the Russian high voltage technology. The first DSRD samples fabricated by VMI showed similar (but no exactly) the same features compared to the Russian DSRD.

The DSRD is a special switching two electrode device [11]. A nanosecond turn OFF mode allows assisting three electrode "slow" switches. Theory and engineering issues for a DSRD design was developed in the 1980s. One can find a description of the DSRD mode of operation in Modulator Pulse Power Conferences in [13]. A DSRD user community is not large and that is why there was not a western supplier of similar devices in the past.

DSRD is a two-terminal dynamic OFF switch. The DSRD impedance is controlled by the following condition

$$\int_0^{t_1} I_{FWD}\,dt = \int_{t_1}^{t_2} I_{RE}\,dt$$

where I_{FWD} and 0 to t_1 are a current and a time interval in a forward diode direction. I_{RE} and $t_2 - t_1$ are a current and an interval in a reverse direction. Special electrical circuits are needed to satisfy mentioned the above condition to control the DSRD switching mode.

Simplified circuit layouts for the DSRD mode operation are shown in Figure 23 where Sw1 (Sw2) represents an initially controlled three electrode switch and K is a kicker. For simplicity, these circuits are associated with a diver to feed one kicker electrode. A symmetrical circuit is needed for the second kicker electrode

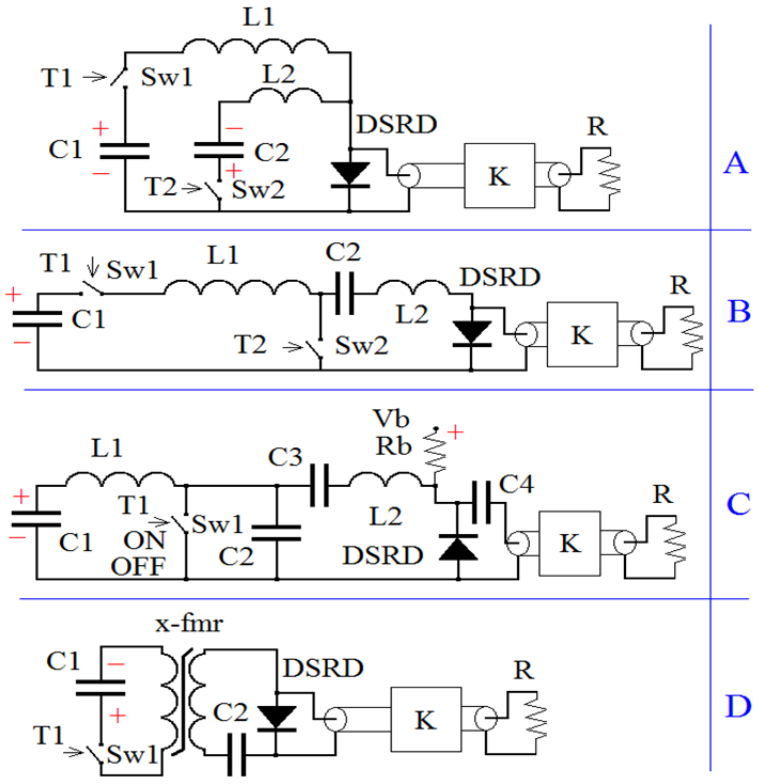

Figure 23: Simplified circuit layouts with the DSRD assistance.

The “A” and “B” drivers require two ON-type switches (Sw1 and Sw2) that are synchronized independently via T1 and T2 triggers. Amplitudes I_{FWD} and I_{RE} depend upon charging voltages, and parameters of L1, C1, L2, and C2 components. The “C” and “D” topologies employ only one primary switch (Sw1). However the “C” driver uses the ON/OFF switch.

A fast MOSFET array is typically used to pump the DSRD stack in this case. The “B” topology is used to generate a waveform with a 0.7/0.8 nsec of rise/fall times (see Figure 25). In this case a single DSRD small dimension crystal was used.

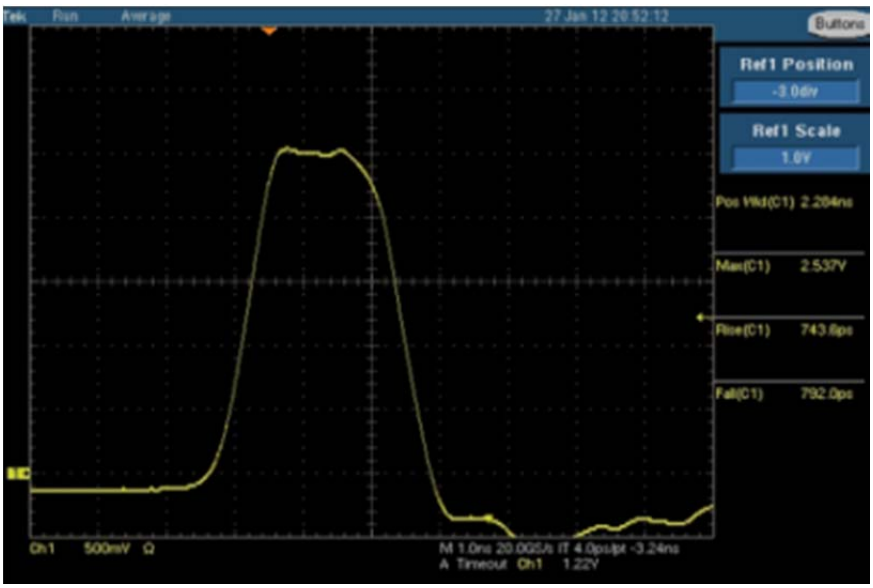

Figure 24: Waveform resulting from a single DSRD crystal. Horizontal scale is 1 nsec/div

This “B” topology can produce nearly a one period of L-Band range (see waveform in Figure 25).

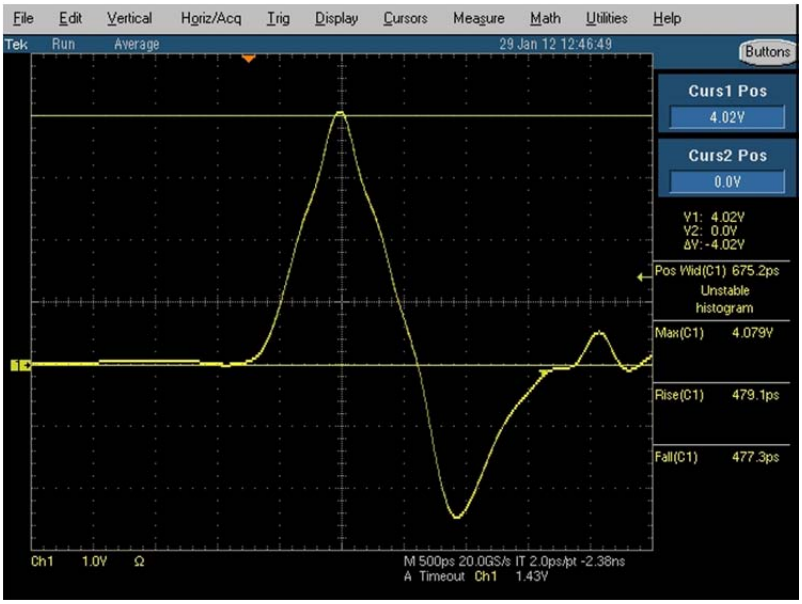

Figure 25: V1=+1200Vpeak and V2=-750Vpeak at 50 Ohm load, horizontal scale is 0.5 nsec/div

This powerful 2 kV/nsec bipolar swing at 50 Ohm resistive load may have a potential application in an advanced digital TFB system.

F) High Rate Pulser Development

A high repetition mode of a 4.0 nsec, 250kW peak power prototype pulser for accelerator applications was developed in the MHz range. The "C" circuit topology was used in this case. A designed solid state switch capable turned off a 200+ A current into a 50 Ohm transmission line. Figure 26 shows a preliminary result of a 2.8 kV, 4.0 nsec pulse on a 50 Ohm load. A measured fall time is 1.2 nsec.

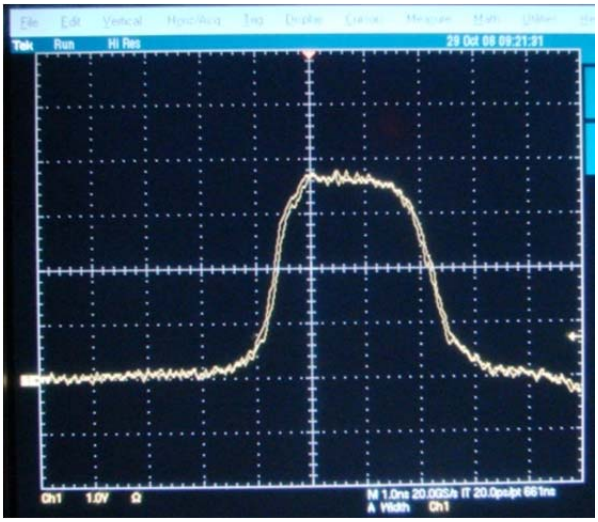

Figure 26: 2.8 kV peak, 4 nsec pulse (at 50 Ohm load). Horizontal scale is 1 nsec/div.

This pulser prototype was tested at 3 MHz repetition rate (see Figure 27 where three pulses separated by a 333 nsec period are shown).

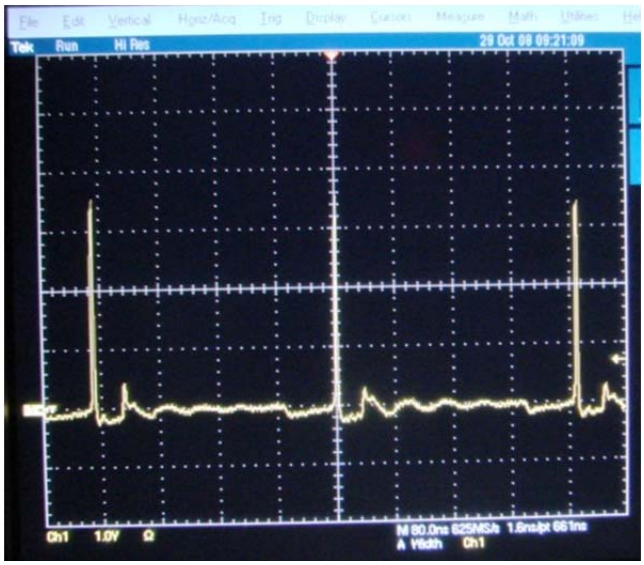

Figure 27: 3 MHz pulse train. Horizontal scale is 80 nsec/div

A level of a residual power between pulses is rather high for the pulser where the “C” topology is used.

A reduction of a residual power is possible if the “B” topology is employed.

Figure 28 shows a 3.5 kV peak pulse with 4.5 nsec FWHM.

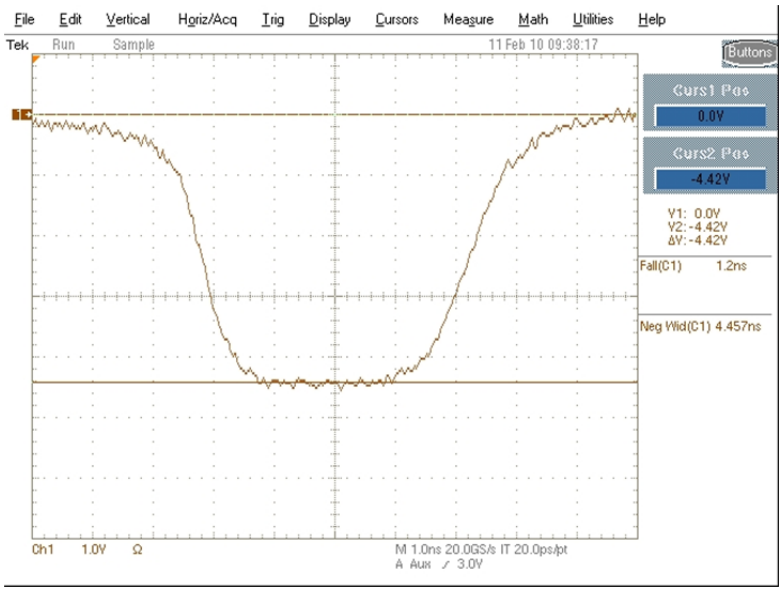

Figure 28: 3.5 kV peak, 4.5 nsec pulse width. Horizontal scale is 1 nsec/div

Pulse “purity” (i.e. the absence of a residual power in the period between of nearest pulses) is a very important parameter for many accelerator applications. Figure 29 shows the purity of a realized power.

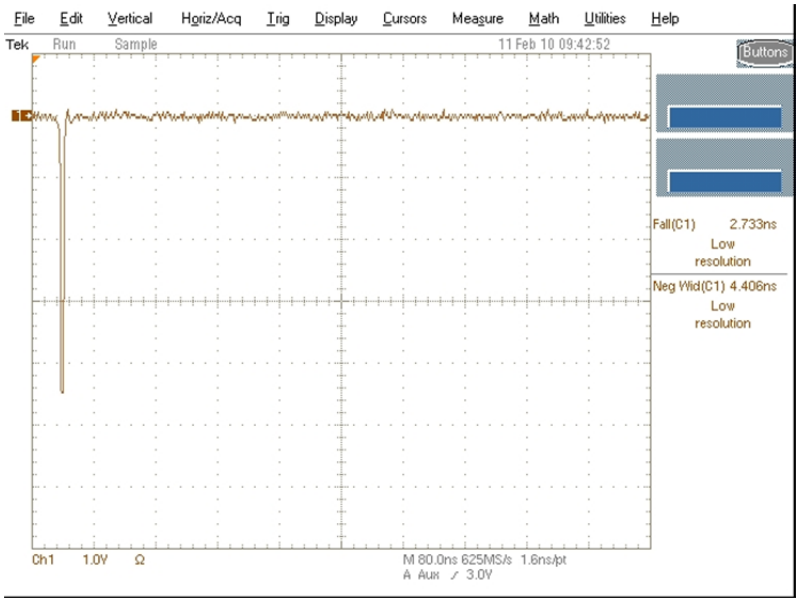

Figure 29: There is no residual energy after pulse. Horizontal scale is 80 nsec/div

The pulse purity depends on many parameters including the circuit topology is used. The “B” pulser topology was used in a 3 MHz repeating mode [14].

Figure 30 shows a 6 nsec FWHM pulse width with a 1 nsec fall time. The amplitude of this pulse is 6 kV peak at a 50 Ohm resistive load. In this case the driver was built according to the “D” circuit layout.

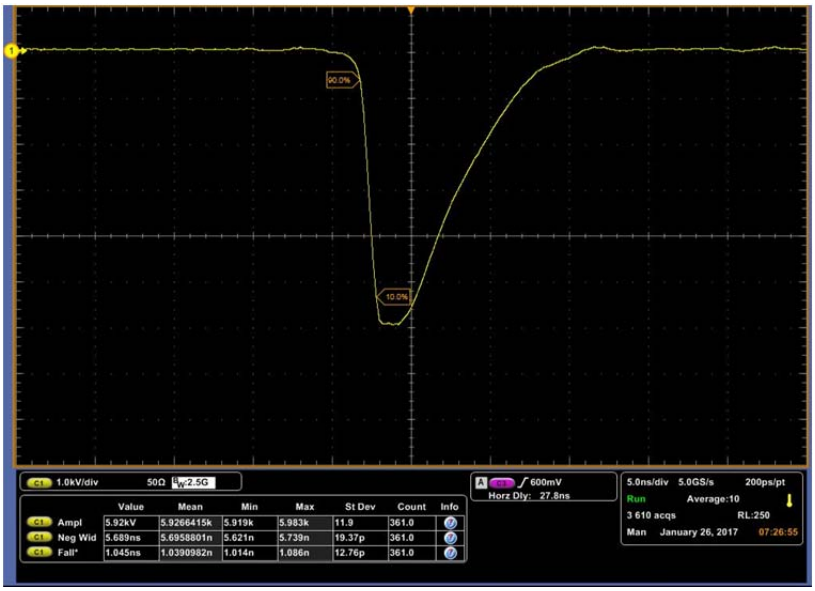

Figure 30: A 6 kV peak, 6 nsec FWHM pulse, horizontal scale is 5 nsec/div (a minor div is 1 nsec)

This assembly has 16 diodes each in this DSRD package. A repletion rate in this circuit was limited by an allowed temperature rise in the magnetic cores of the saturated transformers. A residual power level before and after pulse is shown in Figure 31.

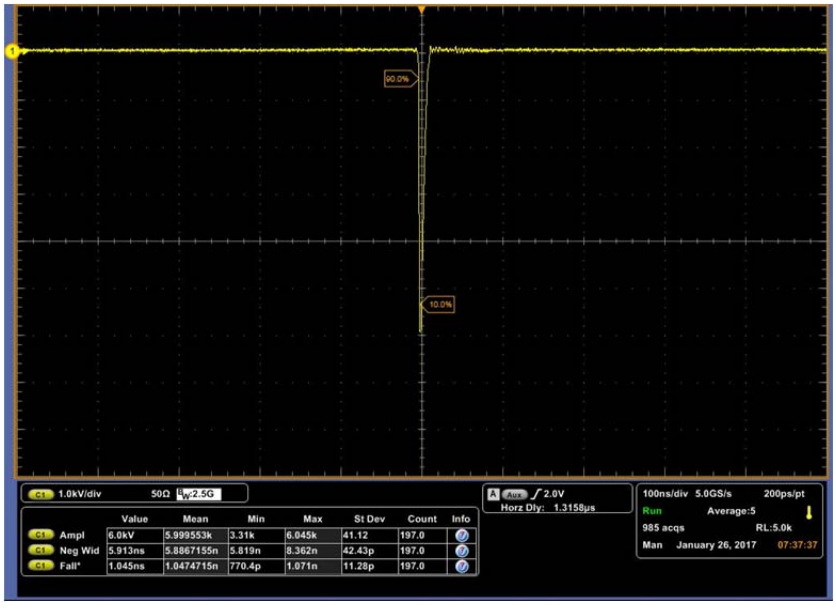

Figure 31: Level of residual voltage before and after 6 kV peak pulse. Horizontal scale is 100 nsec/div

G) Very Short Pulses

In some cases storage ring users require to clean (remove unwanted bunch charges) in the neighboring RF buckets. The FWHM pulse width must be less than 3 nsec. Figure 32 and 33 demonstrate 5.5 kV and 8.6 pulses with FWHM pulse widths <2 nsec and <3 nsec accordingly.

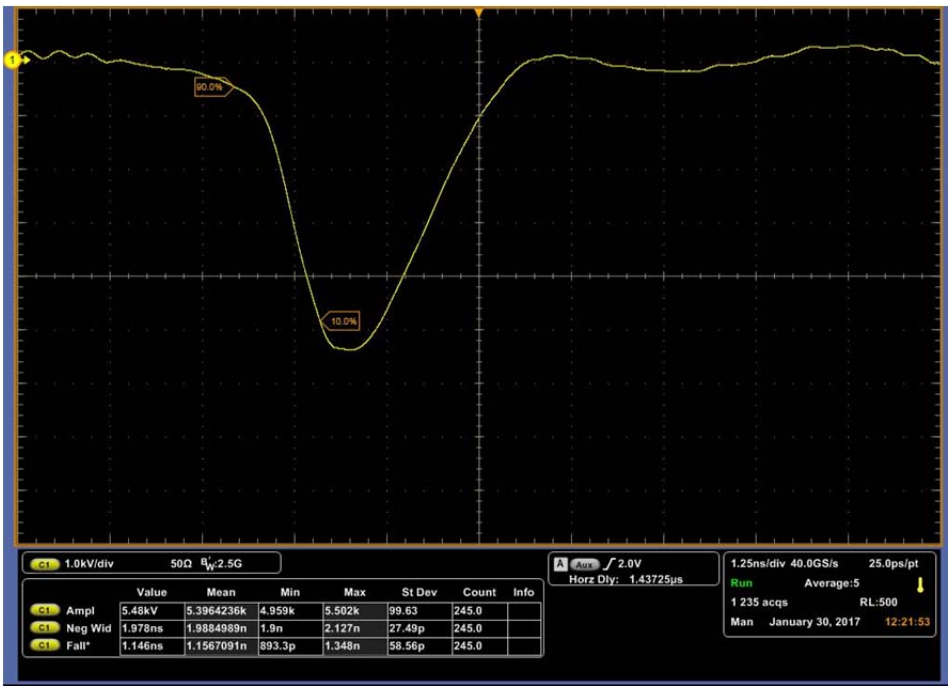

Figure 32: 5.5 kV, 2 nsec pulse. Horizontal scale is 1.25 nsec/div

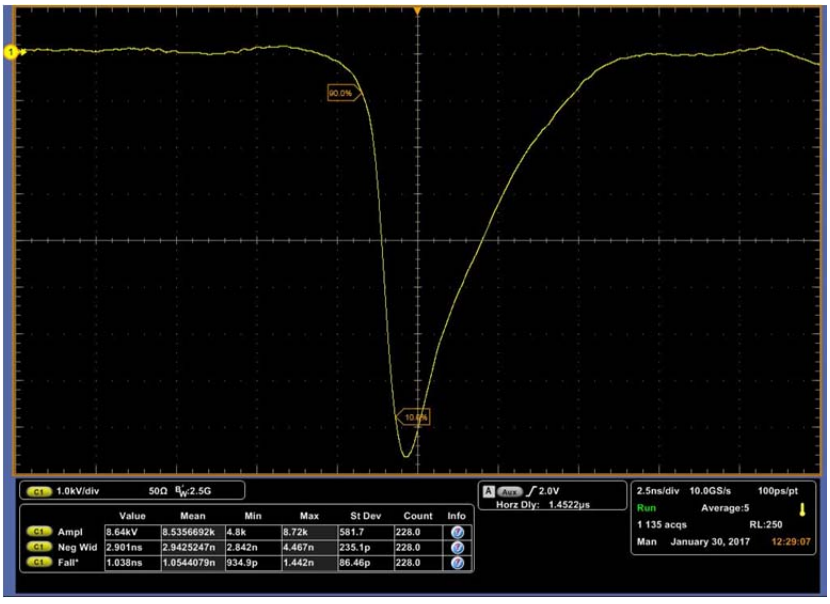

Figure 33: 8.6 kV peak, 3 nsec FWHM pulse with a 1.0 nsec fall time. Horizontal scale is 2.5 nsec/div

The new scheme to upgrade a storage ring require full swap out of the “bad or used” bunch in the train of stored bunches and replace it by a “good” new one. For these cases the driver amplitude has to be more than 15 kV peak and there should be a reasonable pulse plateau to mitigate the potential driver timing errors. A table prototype of an 18 kV peak driver demonstrates the needed waveform that shown in Figure 34.

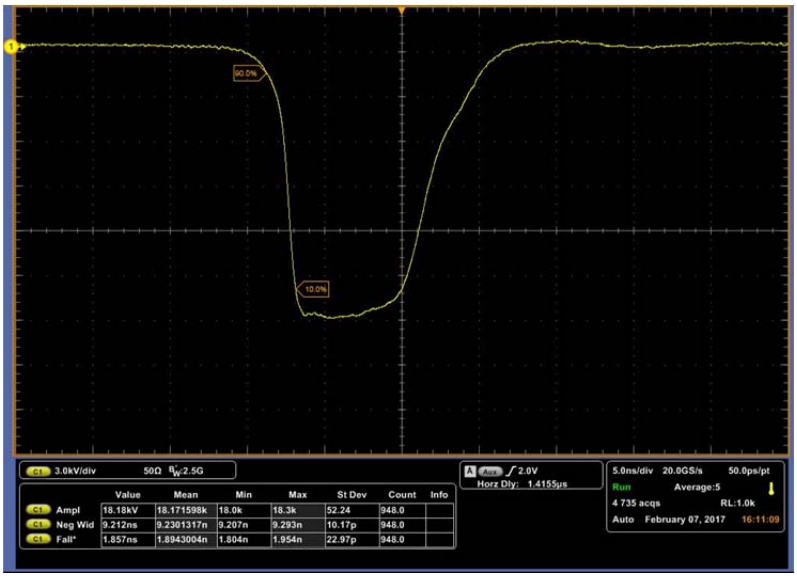

Figure 34: 6.5 MW peak, 9.2 nsec FWHM pulse with a 2.0 nsec fall time. Horizontal scale is 5 nsec/div

There is a rather “slow” process on the end of pulse. A correction is possible by employment of shock wave SW line. Figure 35 shows a 15.5 kV peak, 9.6 nsec FWHM pulse with a 2.1 nsec fall time and 1.9 nsec rise time.

Figure 35: Output waveform where the SW line is employed to form a 1.9 nsec end of the pulse

A level of a residual voltage just before and after the pulse is shown in Figure 36. The residual voltage analysis was not an issue and subject. However it is clear seen that the residual voltage is less than 0.5%.

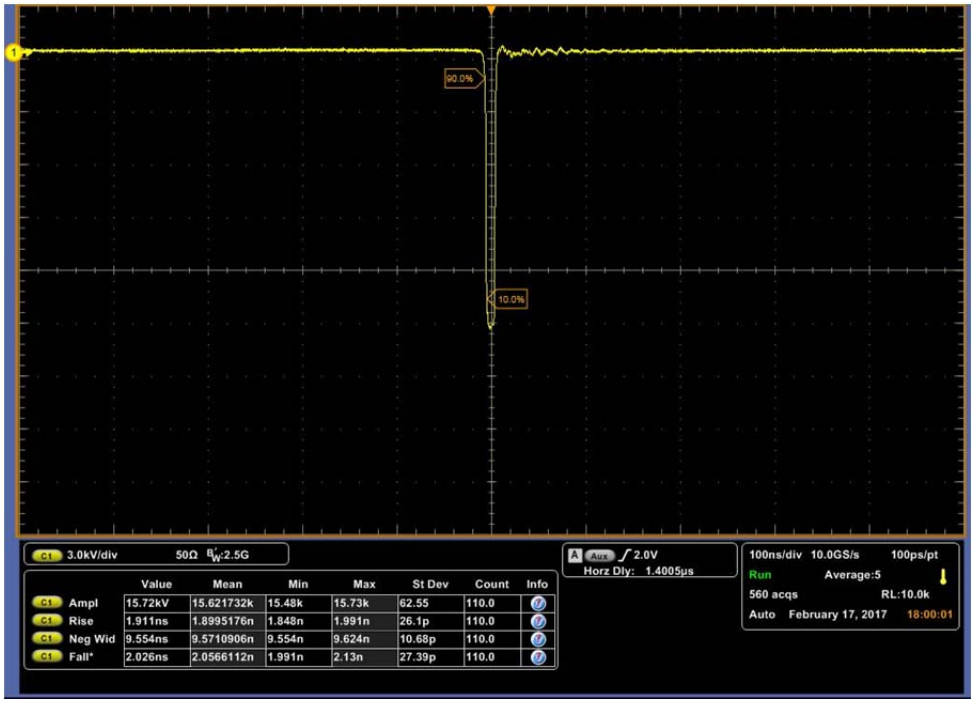

Figure 36: Level of residual power generated by DSRD-based driver with a SW line assistance

In a final, Figure 37 shows a 13 MW peak, 17 nsec FWHM pulse that was formed by DSRD-base pulser.

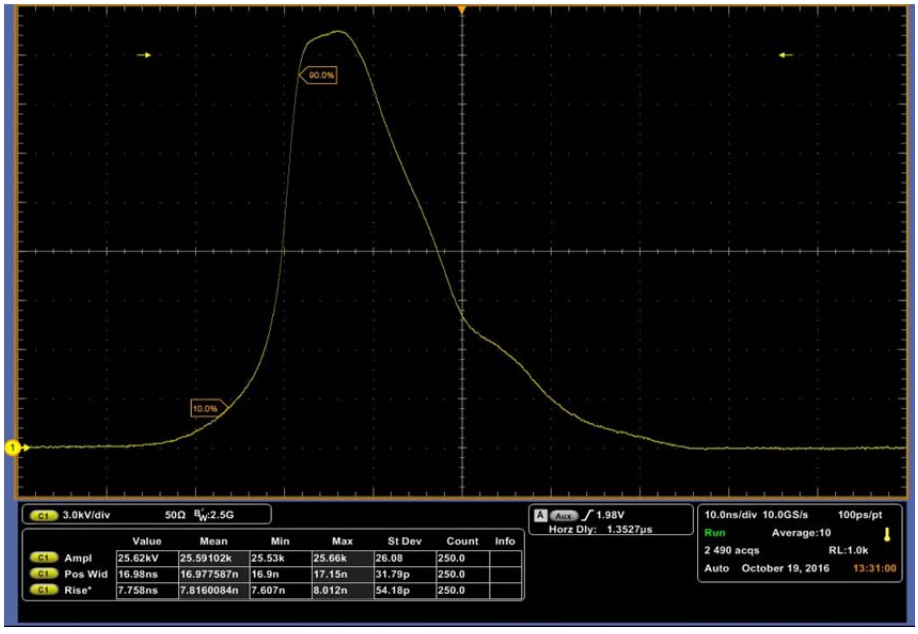

Figure 37: 25.6 kV peak, 17 nsec pulse width at 50 Ohm resistive load, horizontal scale is 10 nsec/div

The pulser here was not optimized from fall/rise times. The pulser was used to check the peak voltage hold off capability of the circuit and diagnostic components. A residual power content of a 25 kV peak pulse is shown in Figure 38.

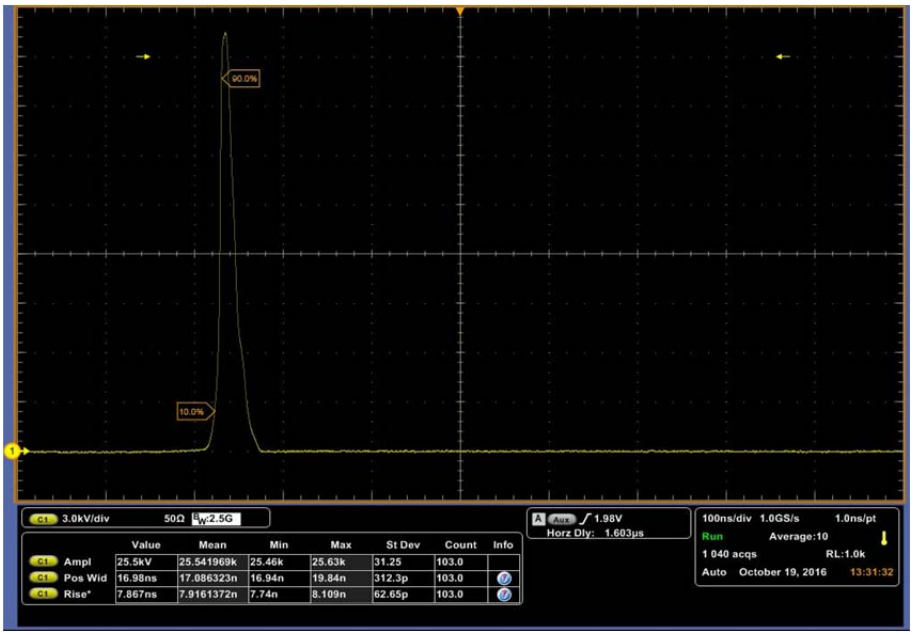

Figure 38: Residual power content of a 25 kV peak pulse. Horizontal scale is 100 nsec/div

Conclusions

Kicker structures:

A brief overview of design and R&D results on TEM-based kicker systems at SLAC was presented. As proposed at SLAC in 2002, the kicker structure described here is still attractive to be developed for a potential realization in the SuperKEKB project. The new kicker structure design will strongly advance the power-handling ability of the TFB feedback kickers for a ring's bunch-by-bunch feedback system.

Fast pulsers:

A brief overview of SLAC R&D results on multi MW nanosecond range driver technologies was discussed. All circuit components are available from industry for obtaining nanosecond, kilovolt pulses. The DSRD-based approach is preferable because, (1) only a low voltage power supply is required to produce a multi-MW nanosecond pulses, and, (2) since the DSRD switch is normally closed, voltage stress is limited by a nanosecond period, hence the susceptibility to hostile environment conditions such as ionizing radiation, mismatches, and strong electromagnetic noise levels is expected to be minimal.

A powerful bipolar L-Band mono pulse was formed with a goal to study a new concept for the TFB system.

A 15.5 kV peak, 9.6 nsec FWHM pulse with 2 nsec fall/rise times at 50 Ohm load was demonstrated in circuit topology where the DSRD and shock wave SW line were employed.

References

[1] D. Goldberg and G. Lambertson, AIP Conference Proceedings #249, 1992, p. 537

[2] https://www1.aps.anl.gov/aps-upgrade

[3] https://als.lbl.gov/als-u/overview/

[4] J. Bradley III, et al. LINAC2016, MOP106016

[5] W. Barry, et al. PAC 1995

[6] A. Krasnykh, SLAC-WP-077,

http://www-public.slac.stanford.edu/sciDoc/docMeta.aspx?slacPubNumber=slac-wp-077

[7] U. Wienands, et. al., EPAC 2004, p. 2843

[8] www.barthelectronics.com

[9] A. Krasnykh, SLAC-PUB-16481, SLAC-WP-130, IPAC2016

[10] R. Haller, et. al., JINR preprint 9-12448, 1979

[11] I. Grekhov et al., Electronics Letters, v. 17, p. 422 (1981)

[12] I.G. Kataev, “Electromagnetic Shock Waves”, 1963

[13] G. Mesyats, Pulsed Power, ISBN 0-306-48654-7, eBook

[14] A. Benwell, et al., SLAC-PUB-15098